IEEE Photonics Journal
An IEEE Photonics Society Publication

Compact Anemometer Using Silver-Coated Fiber Bragg Grating

Volume 4, Number 5, October 2012

Xinyong Dong
Yan Zhou
Wenjun Zhou
Jia Cheng
Zhongdi Su

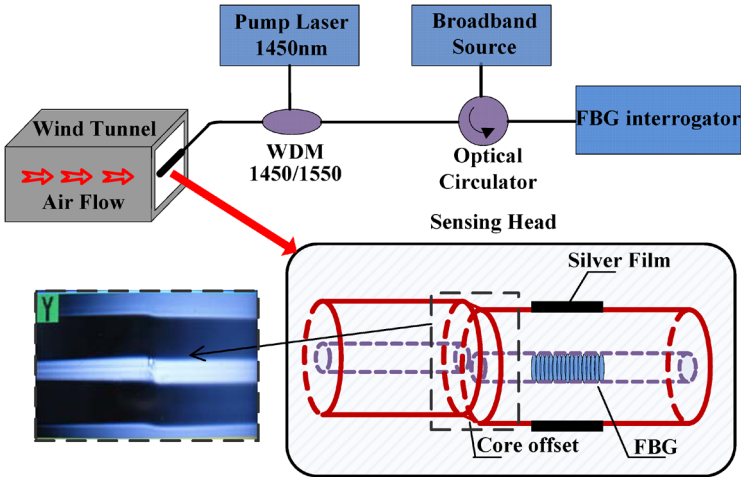

DOI: 10.1109/JPHOT.2012.2208946
1943-0655/$31.00 ©2012 IEEE

Compact Anemometer Using Silver-Coated Fiber Bragg Grating

Xinyong Dong,[1] Yan Zhou,[1,2] Wenjun Zhou,[1,3] Jia Cheng,[2] and Zhongdi Su[4]

[1]Institute of Optoelectronic Technology, China Jiliang University, Hangzhou 310018, China
[2]Zhejiang Province Institute of Metrology, Hangzhou 310013, China
[3]Department of Electronics, Carleton University, Ottawa, Ontario K1S 5B6, Canada
[4]College of Metrology and Measurement Engineering, China Jiliang University, Hangzhou 310018, China

DOI: 10.1109/JPHOT.2012.2208946

Manuscript received June 27, 2012; revised July 8, 2012; accepted July 10, 2012. Date of current version August 1, 2012. This work was supported by the National Basic Research Program of China (973 Program) under Grant 2010CB327804, Qianjiang Talent Project in Zhejiang Province of China under Grant QJD1002002, project supported by the National Science and Technology of China under Grant 2011BAF06B02, project funded by Shanghai Science and Technology Commission of China under Grant 10595812300. Corresponding author: X. Dong (e-mail: xydong@cjlu.edu.cn).

Abstract: An optical fiber thermal anemometer is proposed based on a silver film-coated fiber Bragg grating (FBG) assisted by a core offset fusion splice. Light from a pump laser propagating along the fiber is coupled into the fiber cladding by the splice and absorbed by the silver film to generate heat and increase the temperature of the FBG. Air flow cools down the FBG and its velocity can be measured by the Bragg wavelength shift of the FBG. Experimental results show that the proposed FBG thermal anemometer allows a high resolution of 0.022 m/s in a range up to 6 m/s.

Index Terms: Anemometers, Fiber Bragg gratings, core-offset splice, optical fiber sensors.

1. Introduction

Flow measurement is very important in various areas, such as chemical engineering, marine environment, automotive industry, and process control. A large number of conventional approaches have been explored for detecting the flow field, including electromagnetic measurement, vortex shedding measurement and heat transfer [1]–[3]. Most state-of-the-arts miniaturized flow sensors are based on micro-electro mechanical system (MEMS) technology [4], [5]. These sensors exhibit excellent characteristics such as small size, low power consumption, high sensitivity, fast response, and cost effectiveness. However, these MEMS devices have certain limitations when used in harsh environments such as high electromagnetic interference, high pressure, high vibrations, and radio-active exposure.

Fiber-optic sensors offer a great number of advantages over conventional sensors, such as electrically passive operation, immunity to electromagnetic interference, high sensitivity, integrated structure, and potentially low cost. Recently, fiber flow sensors have attracted more and more research interest [6]–[10]. Most of them are based on optical fiber interferometers, such as fiber Fabry–Pérot interferometer [9] and tapered fiber-based Michelson interferometer [10]. These anemometers measure the velocity inside the duct by traversing the fiber across the flow area so that the air flow affects the interference pattern by bending or distorting the fiber. However, the fiber is easy to break during the measurement.

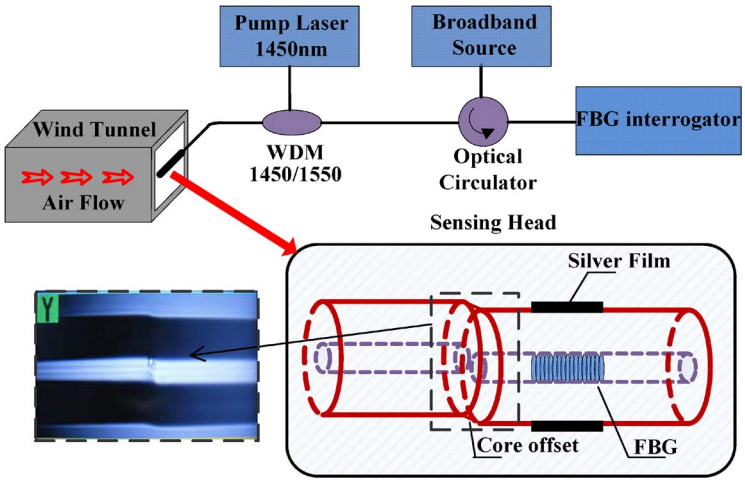

Fig. 1. Set-up of the proposed FBG-based thermal anemometer, with photograph of core-offset splicing point.

Thermal anemometry is a frequently used method in air flow measurement. Conventionally, a high resistance electrical wire is adopted, which is heated by a constant current and cooled by the air flow simultaneously. Air flow velocity is determined from the balanced temperature. Recently, optical fiber flow sensors based on the thermal anemometry method have been reported [11], [12]. The fibers were coated with a metal film and pumped by a high power laser to achieve an initial temperature. To couple the pump laser from the core to the cladding and be absorbed by the metal film, a multimode fiber (MMF) and a long-period fiber grating (LPG) were employed, respectively. The sensing element was a fiber Bragg grating (FBG), whose reflection wavelength was changed with temperature and thus with the air flow velocity. Good results have been achieved but both the MMF and LPG are sensitive to fiber bending that may reduce the coupling efficiency of the pump laser and change the heating effect.

In this paper, an optical fiber thermal anemometer based on a short silver-film-coated FBG collaborating with a core-offset fusion splice is proposed. The core-offset splice couples most of the laser power from the fiber core to the cladding. The silver coating absorbs the pump laser to generate heat and increases the Bragg wavelength of the FBG. When air flows through the anemometer, the anemometer is cooled down and the Bragg wavelength shifts toward the short wavelength direction. As a result, the velocity of the air flow can be measured from the amount of wavelength shift of the FBG.

2. Operation Principle and Sensor Fabrication

A schematic diagram of the proposed FBG-based thermal anemometer is shown in Fig. 1. It consists of a core-offset fusion splice and an FBG coated with a silver film. The FBG, with a length of 4 mm, was written in a hydrogen-loaded single-mode fiber (Corning SMF-28) with a scanning 244-nm UV laser beam through the phase-mask method. It was fusion spliced to another SMF with a core offset of $\sim 5\ \mu$m by using a commercial fusion splicer (FSM-60S) [13]–[15], of which a microscopic photograph is shown in the inset of Fig. 1. The silver film was deposited to the surface of the FBG by using the vacuum evaporating method in two runs with the fiber holder rotated by 180° between the coatings. Due to the limitation of the deposition system, the averaging thickness of the nonuniform film is about 120 nm. A uniform quartz film with a thickness around 100 nm was then deposited over the silver film to prevent it from being oxidized by the airflow.

At the core-offset splicing point, part of the pump laser power was coupled from the lead-in fiber core into the cladding of the FBG and absorbed by the sliver coating. An optical powermeter (JW3208) was used to monitor the transmission power during the splicing process. Evaluated from

the measured transmission loss, ~5 dB, about 70% of the pump laser light was coupled into the cladding of the FBG to heat the silver coating after splicing. This can lead to a sufficient temperature rise in the FBG sensing head. It is important to note that the light propagating in the cladding suffers from a relatively large loss due to the imperfect condition of the cladding-air structure so the distance between the splicing point and the FBG should be kept as short as possible. It was 4 mm in our fabricated sensing head.

As air flows by, part of the heat around the FBG will be taken away and the temperature will be reduced. As a result, a blue shift of the resonant wavelength of the FBG will take place and the wavelength variation depends on the airflow velocity. That makes the measurement. For a given airflow velocity, equilibrium could be achieved between the heating and cooling effects. According to the theories of hot-wire anemometer and heat transfer, the following relationship can be achieved [16]:

$$P_{\text{input}}\varphi a_{\text{Ag}} = [T(v) - T_e](A + B\sqrt{v}) \tag{1}$$

where P_{input} is the input laser power, φ is the coupling coefficient of core-offset splicing point, a_{Ag} is the absorption coefficient of the silver film to pump laser, $T(v)$ is the temperature of the anemometer, T_e is the temperature of the environment, A and B are empirical calibration constant, and v is the wind velocity. The relationship between $T(v)$ and v is therefore given as

$$T(v) = \frac{P_{\text{input}}\varphi a_{\text{Ag}}}{A + B\sqrt{v}} + T_e. \tag{2}$$

The wavelength shift of FBG, $\Delta\lambda$, is dependent on the change of temperature, $\Delta T = T(v) - T(0)$ with $T(0)$ being the temperature of the anemometer when the airflow velocity is zero. This can be described as

$$\Delta\lambda = \lambda_0(\alpha_\Lambda + \xi)\Delta T \tag{3}$$

where λ_0 is the wavelength of the heated FBG without airflow, α_Λ is the thermal expansion coefficient of fiber, and ξ is the thermo-optic coefficient. From Eqs. (2) and (3), we can thus deduce the relationship between the wavelength shift of the FBG and the airflow velocity as

$$\Delta\lambda = -\lambda_0(\alpha_\Lambda + \xi)\frac{P_{\text{input}}\varphi a_{\text{Ag}}}{A\left(1 + \frac{A}{B\sqrt{v}}\right)}. \tag{4}$$

3. Experimental Results and Discussion

A wind tunnel was used to provide stable airflow to the FBG anemometer, which was fixed around the outlet. The dimension of the wind tunnel outlet is 60 cm by 60 cm. The airflow velocity of the wind tunnel can be varied from 0 to 20 m/s. A 1450-nm pump laser with a maximum output power of 450 mW was used to heat the FBG through a 1450/1550 WDM. A broadband source (BBS) with flat output in the wavelength range from 1525 to 1560 nm and an FBG interrogator with a wavelength resolution of 1 pm were used to monitor the reflection wavelength of the FBG via an optical circulator.

To examine the performance of the FBG anemometer, several tests were conducted. Fig. 2(a) shows the reflection spectra of FBG before and after the pump laser was turned on. The FBG's reflection spectrum shifted to the longer wavelength direction for ~0.6 nm due to the heating effect of the pump laser. The reflectivity was reduced slightly and the reflection profile changed a bit. This is related to the nonuniform heating effect by the pump laser along the length of the FBG. The power of pump laser was reduced gradually along the FBG due to the continuous absorption by the sliver film. That made the heating effect, hence the temperature and the period of the FBG, was reduced gradually along the FBG. As a result of this minor chirping effect, the FBG's reflectivity was reduced and the spectrum was changed. The FBG used in the experiment is relatively short, resulting in wide bandwidth and low reflectivity. So in this work, we get the resonant wavelength

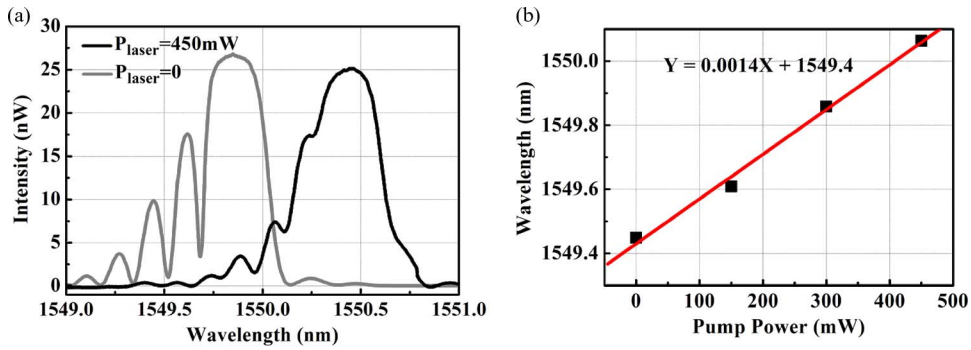

Fig. 2. (a) Reflection spectra of the FBG anemometer with and without laser pumping. (b) Wavelength shift of the FBG against power of the pump laser.

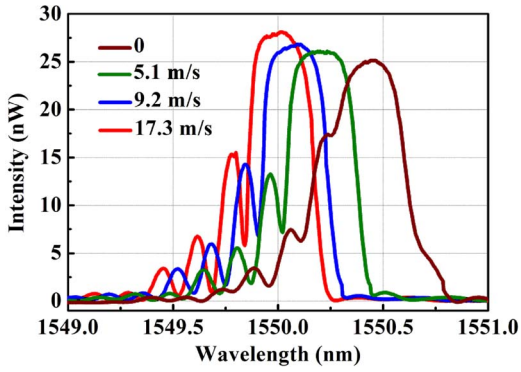

Fig. 3. Reflection spectra of the FBG anemometer under various airflow velocities.

shift through monitoring the peak resonance adjacent to the Bragg peak (center wavelength). Fig. 2(b) shows the resonant wavelength shift with increasing power of the 1450-nm pump laser. It can be seen that the wavelength shift is proportional to the power of the pump laser. The slope is 1.4 pm/mW.

The measurement of airflow velocity was processed under the fixed pump laser power of 450 mw. We change the airflow velocity in a wide range. Fig. 3 shows the reflection spectra of the FBG anemometer under different airflow velocities. It shows that the wavelength of the FBG experienced a gradual blue-shift with the increase of airflow velocity. This is because the heat was partially carried away by the airflow and hence temperature was reduced gradually with increasing the airflow velocity. The measurement was carried out at room temperature, $\sim$20 °C, to avoid any possible influences of the environmental temperature variations on the measurements. It is also noticed that with increase of the airflow velocity, the reflectivity was increased slightly and the spectral profile changed a bit back to the original one. This is because the chirping effect was relieved gradually along with the decrease of temperature with airflow velocity.

The measured wavelength of the FBG anemometer as a function of the airflow velocity is shown in Fig. 4. The total wavelength shift is $\sim$0.45 nm when the airflow velocity is changed from 0 to 17.3 m/s. It can be seen that the response is nearly linear when the airflow velocity is less than 6 m/s, as shown in the inset of Fig. 4. The sensitivity is 45.3 pm/(m/s). When the air flow velocity is over 6 m/s, the response becomes smaller and smaller. There is an obvious saturation phenomenon because the temperature becomes closer to the room temperature and the available heat is becoming less with increasing the airflow velocity. Assuming that the thermal sensitivity of the FBG is 10.7 pm/°C, the temperature of the anemometer would be $\sim$15 °C higher than room temperature

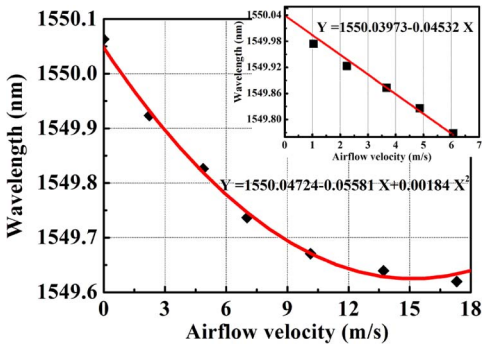

Fig. 4. Resonant wavelength versus applied airflow velocity. The inset shows the results for airflow velocity less than 6 m/s.

at the airflow velocity of 17.3 m/s. However, this linear response range can be broadened by increasing the pump laser power.

Based on the wavelength resolution of the FBG interrogator, 1 pm, and the achieved sensitivity, 45.3 pm/(m/s), the resolution for airflow velocity measurement is up to 0.022 m/s. It is about 4 times higher than that of the previously-reported FBG anemometer by using a long-period grating [6], and comparable with that of the cobalt-doped fiber Bragg grating anemometer [9].

4. Conclusion

A highly sensitive anemometer has been demonstrated by combining a silver-film-coated FBG with a core-offset fusion splice. A pump laser at 1450 nm with a maximum output power of 450 mW was used to heat the FBG through the fusion splice. The airflow velocity was measured by monitoring the wavelength shift of the FBG. The measurement range is up 17.3 m/s. A linear response of 45.3 pm/(m/s) and a high resolution of 0.022 m/s have been achieved for the airflow velocity below 6 m/s. The demonstrated thermal anemometer is simple in structure and easy for manufacture, with potentially low cost.

References

[1] J. E. Cha, Y. C. Ahn, and M. H. Kim, "Flow measurement with an electromagnetic flowmeter in two-phase bubbly and slug flow regimes," *Flow Meas. Instrum.*, vol. 12, no. 5, pp. 329–339, 2002.
[2] A. Venugopal, A. Agrawal, and S. V. Prabhu, "Review on vortex flowmeter-Designer perspective," *Sens. Actuators A, Phys.*, vol. 170, no. 1/2, pp. 8–23, Nov. 2011.
[3] P. Ligeza, "An investigation of a constant-bandwidth hot-wire anemometer," *Flow Meas. Instrum.*, vol. 20, no. 3, pp. 116–121, Jun. 2009.
[4] A. Rasmussen and M. E. Zaghloul, "In the flow with MEMS," *IEEE Circuits Devices Mag.*, vol. 14, no. 4, pp. 12–25, Jul. 1998.
[5] S. Oda, M. Anzai, S. Uematsu, and K. Watanabe, "A silicon micromachined flow sensor using thermopiles for heat transfer measurements," *IEEE Trans. Instrum. Meas.*, vol. 52, no. 4, pp. 1155–1159, Aug. 2003.
[6] C. Jewart, B. McMillen, S. K. Cho, and K. P. Chen, "X-probe flow using self-powered active fiber Bragg gratings," *Sens. Actuators A, Phys.*, vol. 127, no. 1, pp. 63–68, Feb. 2006.
[7] G. D. Byrne, S. W. James, and R. P. Tatam, "A Bragg grating based fibre optic reference beam laser Doppler anemometer," *Meas. Sci. Technol.*, vol. 12, no. 7, pp. 909–913, Jul. 2001.
[8] V. Lien and F. Vollmer, "Microfluidic flow rate detection based on integrated optical fiber cantilever," *Lab Chip*, vol. 7, no. 10, pp. 1352–1356, Oct. 2007.
[9] C. L. Lee, W. Y. Hong, H. J. Hsieh, and Z. Y. Weng, "Air gap fiber Fabry-Pérot interferometer for highly sensitive micro-airflow sensing," *IEEE Photon. Technol. Lett.*, vol. 23, no. 13, pp. 905–907, Jul. 2011.
[10] Y. L. Hsiao, C. M. Li, T. C. Chiang, and C. L. Lee, "A novel airflow sensor based on a reflective tapered fiber interferometer," in *Proc. OECC*, 2011, pp. 709–710.
[11] L. J. Cashdollar and K. P. Chen, "Fiber Bragg grating flow sensors powered by in-fiber light," *IEEE Sensors J.*, vol. 5, no. 6, pp. 1327–1331, Dec. 2005.
[12] P. Caldas, P. A. S. Jorge, G. Rego, O. Frazão, J. L. Santos, L. A. Ferreira, and F. Araújo, "Fiber optic hot-wire flowmeter based on a metallic coated hybrid long period grating/fiber Bragg grating structure," *Appl. Opt.*, vol. 50, no. 17, pp. 2738–2743, Jun. 2011.

[13] T. Guo, H. Y. Tam, P. A. Krug, and J. Albert, "Reflective tilted fiber Bragg grating refractometer based on strong cladding to core recoupling," *Opt. Exp.*, vol. 17, no. 7, pp. 5736–5742, Mar. 2009.
[14] C. Gouveia, P. A. S. Jorge, J. M. Baptista, and O. Frazão, "Temperature-independent curvature sensor using FBG cladding modes based on a core misaligned splice," *IEEE Photon. Technol. Lett.*, vol. 23, no. 12, pp. 804–806, Jun. 2011.
[15] W. J. Zhou, Y. Zhou, X. Y. Dong, L. Y. Shao, J. Cheng, and J. Albert, "Fiber-optic curvature sensor based on cladding-mode Bragg grating excited by fiber multimode interferometer," *IEEE Photon. J.*, vol. 4, no. 3, pp. 1051–1057, Jun. 2012.
[16] S. R. Gao, A. P. Zhang, H. Y. Tam, L. H. Cho, and C. Lu, "All-optical fiber anemometer based on laser heated fiber Bragg gratings," *Opt. Exp.*, vol. 19, no. 11, pp. 10 124–10 130, May 2011.